

Supplementary Table 1. Strains used in this study.

Strain	Genotype, Description	Source (Reference)
<i>E. coli</i> DH5α	<i>E. coli</i> host for general cloning	Life Technologies
<i>E. coli</i> BL21(DE3)	<i>E. coli</i> host for protein production	Life Technologies
<i>E. coli</i> BL21(DE3)-Gold	<i>E. coli</i> host for protein production	Stratagene/Agilent
<i>E. coli</i> BW25113/pIJ790	<i>E. coli</i> host for λRED-mediated PCR targeting	(1)
<i>E. coli</i> DH5α/BT340	<i>E. coli</i> host for FLP-mediated excision of disruption cassette	(2)
<i>E. coli</i> ET12567/pUZ8002	Methylation-deficient <i>E. coli</i> host for intergeneric conjugation	(3)
<i>S. platensis</i> SB12029	CB00739 $\Delta ptmR1$ (markerless)	(4)
<i>S. platensis</i> SB12037	SB12029 $\Delta ptmA1::aac(3)IV$	This study
<i>S. platensis</i> SB12038	SB12029 $\Delta ptmA2::aac(3)IV$	This study

Supplementary Table 2. Plasmids and cosmids used in this study.

Plasmid	Description	Source (Reference)
pBS12064	Cosmid 17E7 containing a partial <i>ptm</i> gene cluster	This study
pBS12065	pBS12064 $\Delta ptmA1::aac(3)IV$	This study
pBS12066	pBS12064 $\Delta ptmA2::aac(3)IV$	This study
pBS3080	pRSFDuet-1 derived plasmid containing a <i>Bsm</i> FI site for ligation-independent cloning (LIC) and encodes a TEV protease site after the N-terminal His ₆ -tag	(5)
pBS12067	pBS3080 harboring the full length <i>ptmA2</i> ; used for enzyme assays	This study
pBS12068	pBS12067-derived <i>ptmA2</i> H215A mutant	This study
pBS12069	pBS12067-derived <i>ptmA2</i> E416A mutant	This study
pBS12070	pBS12067-derived <i>ptmA2</i> A497K mutant	This study
pBS12071	pBS12067-derived <i>ptmA2</i> T171SGTSGRPK mutant	This study
pBS12072	pBS12067-derived <i>ptmA2</i> A497K/T171SGTSGRPK mutant	This study
pBS12073	pBS12067-derived <i>ptmA2</i> T406R/T408K mutant	This study
pMCSG68	LIC plasmid that encodes a TEV protease site after the N-terminal His ₆ - and StrepII-tags, and the tRNA genes, <i>argU</i> and <i>ileX</i> , for rare codons	(6)
pBS12074	pMCSG68 harboring full length <i>ptmA2</i> ; used for crystallography	This study

Supplementary Table 3. Primers used in this study.

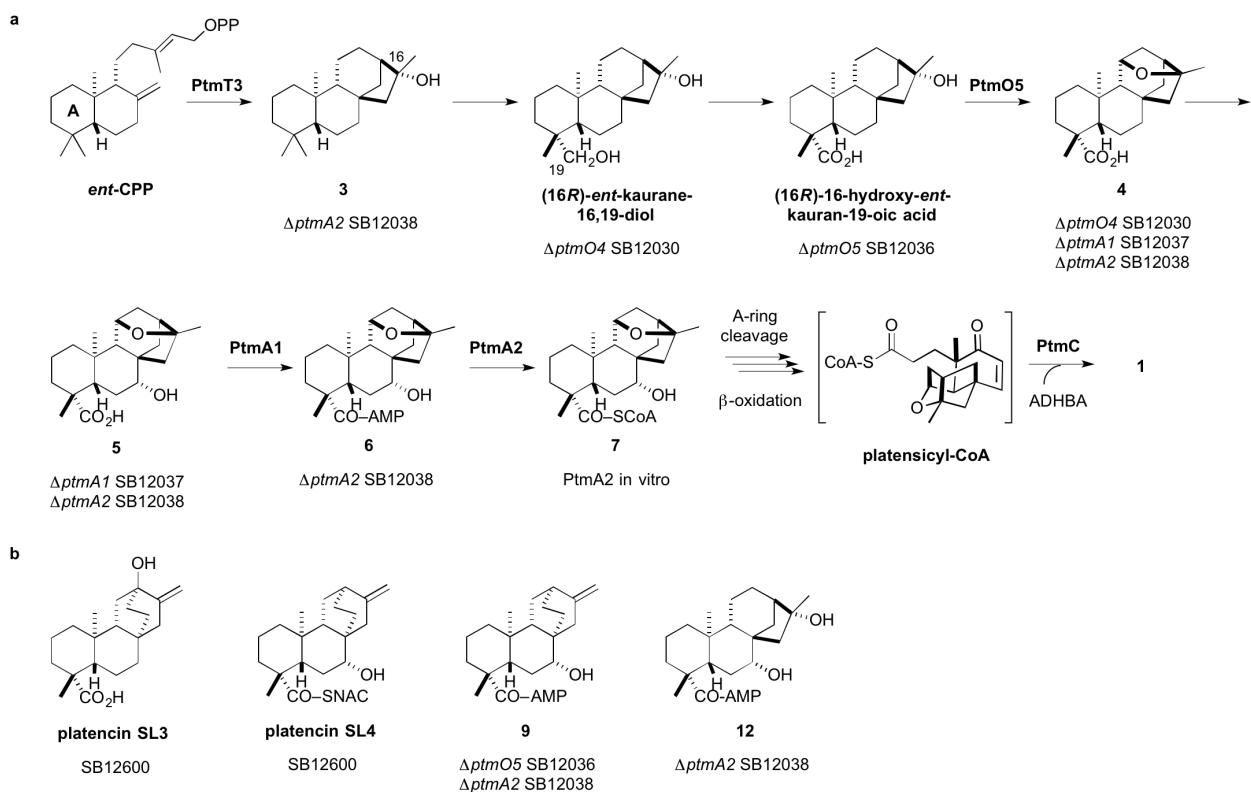
Primer	Nucleotide Sequence (5'-3')	Function
739A1KO_F	GGTACCTGAAGGTAAGGGAGAGCCATGC CCGACAGAGAGATTCCGGGGATCCGTCGA CC	PCR targeting for <i>ptmA1</i> inactivation
739A1KO_R	CCAGGGATTCCCGTTCGTACCATCATGACC TCACCACTCGTGTAGGCTGGAGCTGCTTC	PCR targeting for <i>ptmA1</i> inactivation
739A1ID_F	CCTGAAGGTAAGGGAGAGCC	PCR confirmation
739A1ID_R	TGACCTCACCACTCGTGTCA	PCR confirmation
739A1south_F	CACCGTAGTCGTCGAAGTA	Southern probe
739A1south_R	CCTTCAGGTACCTAACCCGC	Southern probe
739A2KO_F	GTCCCCGACCGCCTAGGAGCCACCTTGCA GCACACGACCATTCCGGGGATCCGTCGAC C	PCR targeting for <i>ptmA2</i> inactivation
739A2KO_R	ATCACGGGCTGCCGGTCACTCATCTCAGC GCCCGGGGCGCTGTAGGCTGGAGCTGCTTC	PCR targeting for <i>ptmA2</i> inactivation
739A2ID_F	ACTTCACCGACCTGTTCAC	PCR confirmation
739A2ID_R	CTGCCGGTCACTCATCTCAG	PCR confirmation
739A2south_F	GGTGGTGCCGAACTCATACA	Southern probe
739A2south_R	CATTACCGCGACCGAACAG	Southern probe
739A2_F	AAAACCTCTATTCCAGTCGTTGCAGCAC ACGACCATC	<i>ptmA2</i> amplification for pBS3080
739A2_R	TACTTACTTAAATGTTATCAGCGCCGGG GCCGAG	<i>ptmA2</i> amplification for pBS3080
H215A_F	GGCCCCATGTTGCCATCGGCAACCAC	Mutagenesis
H215A_R	GTGGTTGCCGATGGCGAACATGGGGCC	Mutagenesis
E416A_F	AAGTCGGCGGCCGGAACATCTTCCCG	Mutagenesis
E416A_R	CGGGAAGATGTTGCCGCCGCCGACTT	Mutagenesis
A497K_F	ACCGTGTGGGCAAACGGGACTACGAC	Mutagenesis
A497K_R	GTCGTAGTCCCCTTGCCCCACACGGT	Mutagenesis
T171SGTSGRPK_F (P-loop_F)	CCCGTCCTGTCCTGTACACCAGCGGCACC AGCGGGCGGCCGAAA	Mutagenesis
T171SGTSGRPK_R (P-loop_R)	TTTCGGCCGCCCGCTGGTGCCGCTGGTGT ACAGGACAGGACGGG	Mutagenesis
T406R/T408K_F	ACCTTCCTCGGCCGTACGAAACGGATGCT CAAG	Mutagenesis
T406R/T408K_R	CTTGAGCATCCGTTCGTACGGCCGAGGA AGGT	Mutagenesis
739xtalA2_F	TACTTCCAATCCAATGCCTTGCAGCACAC GACCATCGGCGACGTC	<i>ptmA2</i> amplification for pMCSG68
739xtalA2_R	TTATCCACTTCCAATGTTAGCGCCCGGGG CCGAGCGTC	<i>ptmA2</i> amplification for pMCSG68

Supplementary Table 4. Data collection and refinement statistics^a

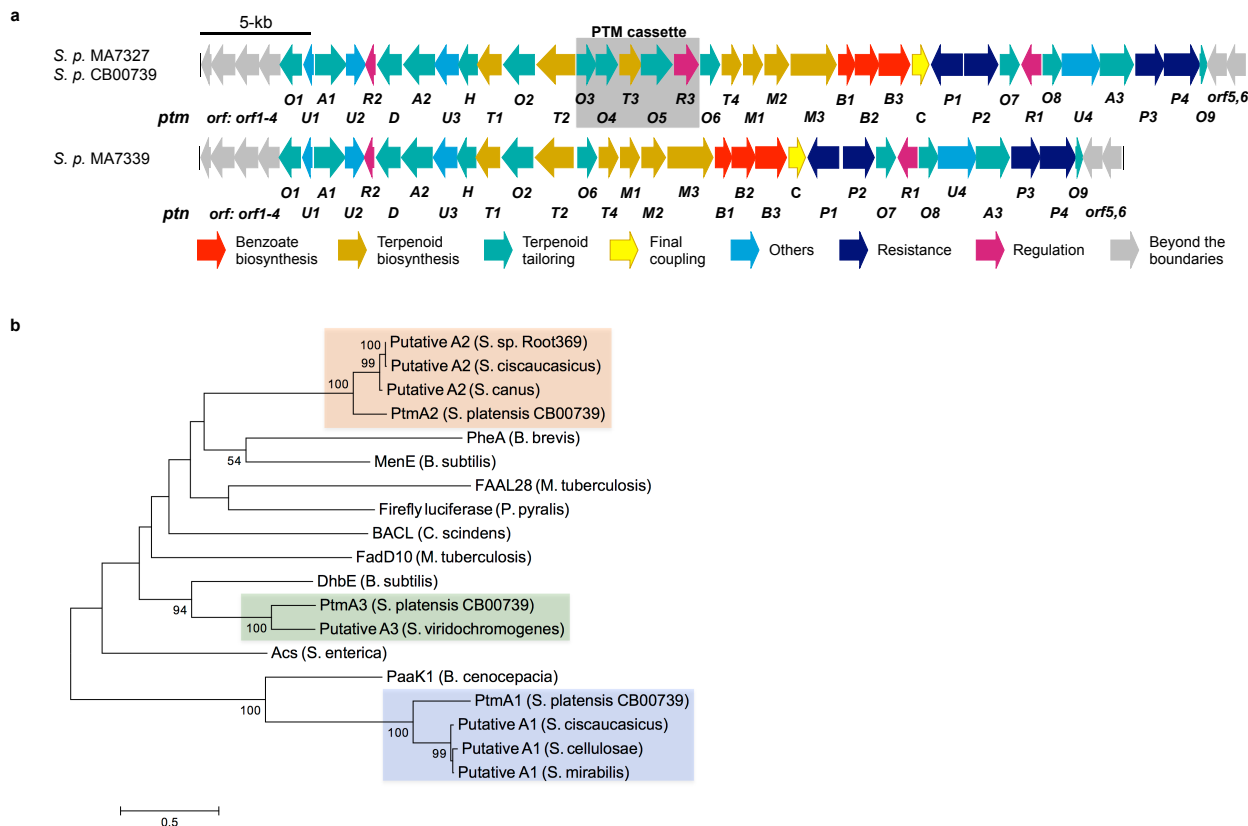
	PtmA2, 5E7Q	PtmA2/ 12 , 5UPQ	PtmA2/ 6 , 5UPS	PtmA2/ 11 , 5UPT
Data collection				
Space group	P2 ₁ 2 ₁ 2 ₁	P2 ₁ 2 ₁ 2 ₁	P3 ₁ 21	P4 ₃ 2 ₁ 2
Cell dimensions				
<i>a, b, c</i> (Å)	70.87, 146.89, 146.93	69.61, 145.74, 145.76	162.67, 162.67, 114.14	146.16, 146.16, 71.14
α, β, γ (°)	90, 90, 90	90, 90, 90	90, 90, 120	90, 90, 90
Resolution (Å)	50.0–2.23 (2.27–2.23)	38.5–2.42 (2.46–2.42)	50.0–2.05 (2.09–2.05)	50.0–1.92 (1.95–1.92)
Unique reflections	75465 (3753)	57650 (2822)	108962 (5391)	59353 (2866)
<i>R</i> _{merge}	9.4 (70.1)	12.3 (90.9)	11.5 (89.3)	9.7 (84.1)
<i>R</i> _{meas}	10.3 (80.6)	13.3 (98.2)	12.2 (95.1)	10.3 (92.6)
<i>I</i> / σ <i>I</i>	23.0 (1.95)	18.7 (2.2)	24.6 (2.05)	26.1 (2.2)
Completeness (%)	100 (99.9)	99.7 (99.5)	100 (100)	99.5 (98.7)
Redundancy	6.1 (4.1)	7.1 (7.0)	8.6 (8.5)	9.0 (5.9)
CC _{1/2} (Å)	0.697	0.617	0.749	0.660
CC*	0.906	0.873	0.926	0.892
Refinement				
Resolution (Å)	48.3–2.23 (2.231–2.289)	38.5–2.42 (2.474–2.412)	48.3–2.05 (2.103–2.05)	36.2–1.92 (1.965–1.916)
No. reflections	71661 (5177)	54772 (3815)	103541 (7514)	56197 (4023)
<i>R</i> _{work} / <i>R</i> _{free}	17.3/20.6 (25.2/27.3)	23.2/28.5 (28.6/38)	15.6/18.8 (22.5/25.3)	16.4/19.6 (25.2/29.4)
No. atoms				
Protein	7896	7670	8008	3978
Ligand/ion	107	166	124	100
Water	357	212	722	378
<i>B</i> -factors				
Protein	43.6	47.4	40.0	30.4
Ligand/ion	75.2	50.6	37.2	49.0
Water	44.3	42.0	48.3	42.0
R.m.s. deviations				
Bond lengths (Å)	0.011	0.009	0.011	0.013
Bond angles (°)	1.403	1.351	1.513	1.65
Ligands RSCC	–	2 molecules of 12 (1 per chain, <i>A</i> = 0.95, <i>B</i> = 0.95)	2 molecules of 6 (1 per chain, <i>A</i> = 0.98, <i>B</i> = 0.98)	3 molecules of 11 (8JG ₇₀₁ = 0.82, 8JG ₇₀₂ = 0.85, 8JG ₇₀₃ = 0.82)

^a Data were collected from a single crystal for each structure. Values in parentheses are for highest-resolution shell.

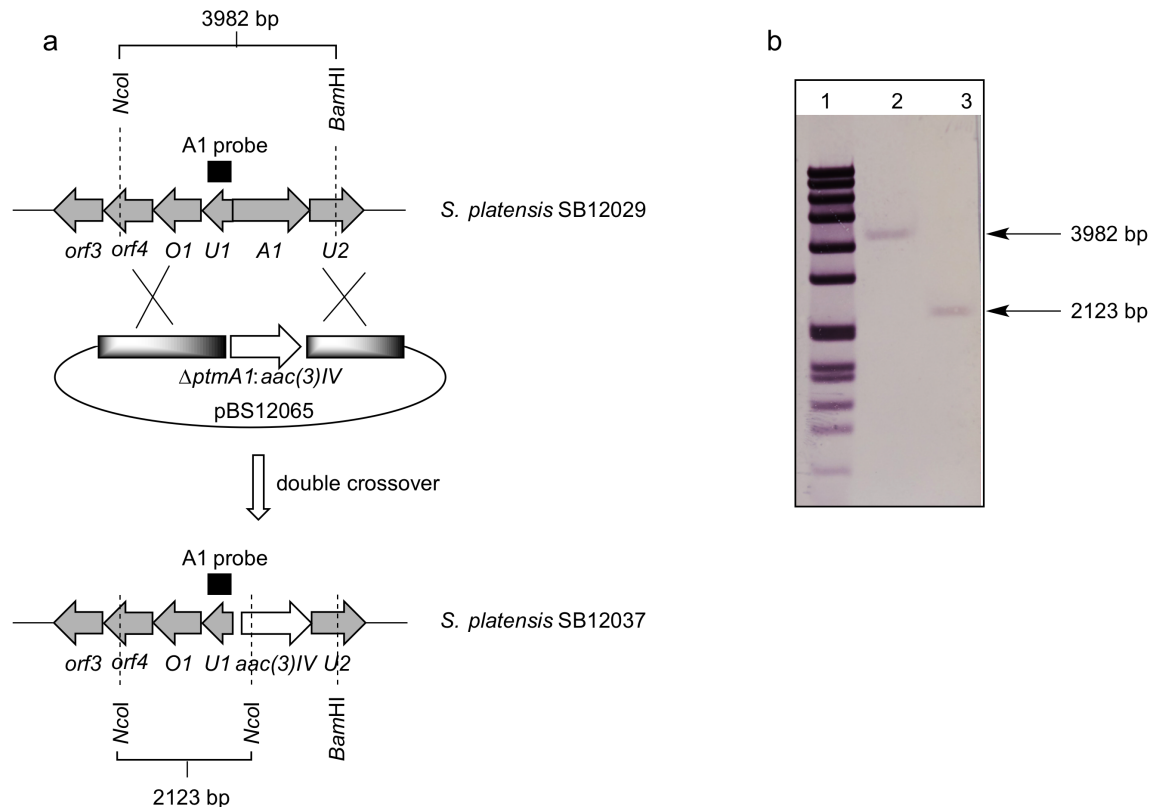
Supplementary Figure 1. The unified biosynthetic pathway of PTM and PTN. (a) The *ptm* biosynthetic gene cluster encodes the genes necessary for production of both PTM and PTN. The early steps of PTM biosynthesis are shown with isolated intermediates and the recombinant strains that produced each compound listed^{4,7,8}. Carboxylic acid activation with CoA by PtmA1 and PtmA2 occurs before A-ring cleavage and β -oxidation. After platensicyl-CoA is formed, PtmC catalyzes the coupling of ADHBA to form PTM (**1**). The biosynthesis of PTN from *ent*-coparyl diphosphate (CPP) parallels PTM with the exception of the PtmT1-catalyzed formation of *ent*-atiserene, which undergoes similar transformations except for PtmO5, to afford platencinyl-CoA, which is coupled with ADHBA to form PTN (**2**). (b) Selected PTM and PTN intermediates or congeners supporting early activation of the C-19 methyl group.



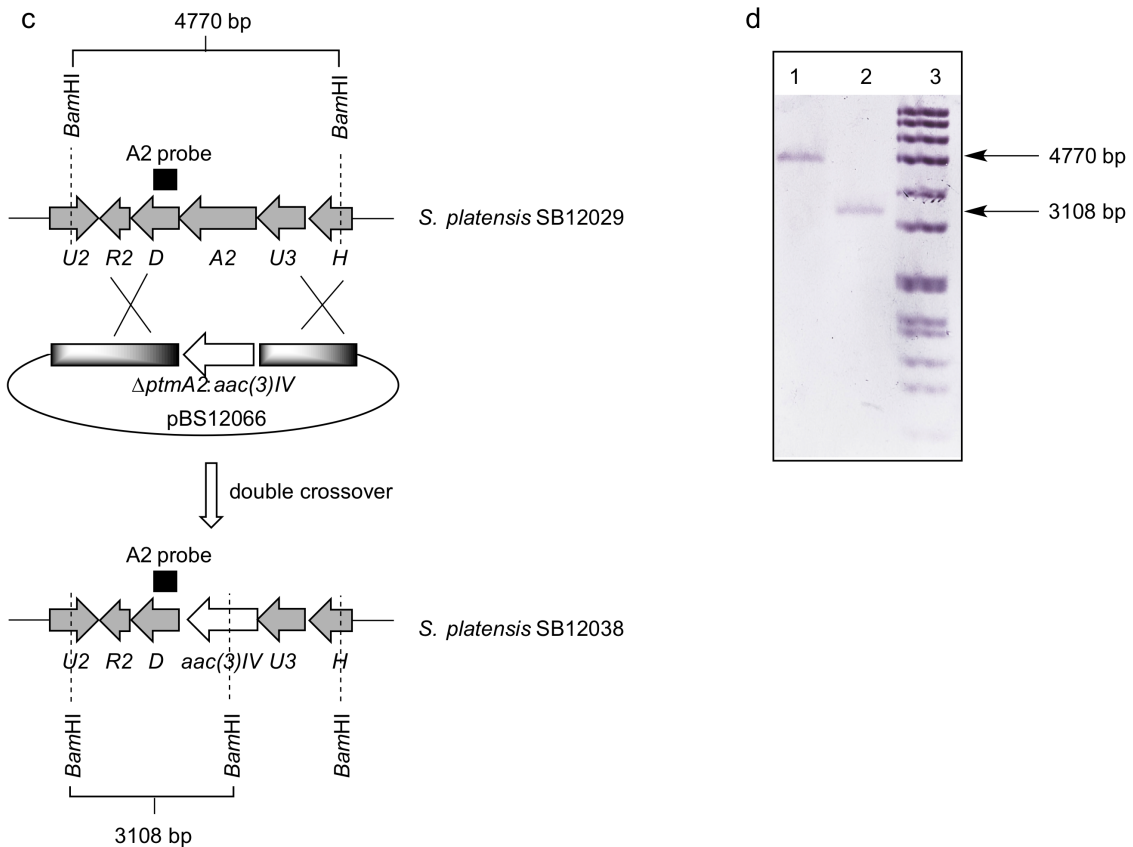
Supplementary Figure 2. The *ptm* and *ptn* biosynthetic gene clusters. (a) Genetic organization of the *ptm* gene clusters from the dual PTM–PTN producers *S. platensis* MA7327 and *S. platensis* CB00739 and the *ptn* gene cluster from the PTN-only producer *S. platensis* MA7339^{9,10}. The PTM–PTN dual overproducer *S. platensis* SB12029 used in this study to construct the $\Delta ptmA1$ and $\Delta ptmA2$ overproducers *S. platensis* SB12037 and SB12038, respectively, was previously constructed by in-frame deletion of the pathway-specific negative regulator *ptmR1* in *S. platensis* CB00739⁴. The three acyl-CoA synthetases discussed in this study, PtmA1, PtmA2, and PtmA3, are encoded by genes in both the *ptm* and *ptn* gene clusters. (b) Phylogenetic tree of PtmA1, PtmA2, PtmA3, and selected members of the ANL superfamily of adenylating enzymes. Bootstrap values >50 (based on 1000 resampled trials) are given at nodes. Bar, 0.5 substitutions per amino acid position. PtmA1, PtmA2, and PtmA3 with selected homologues are shaded in blue, peach, and green boxes, respectively.



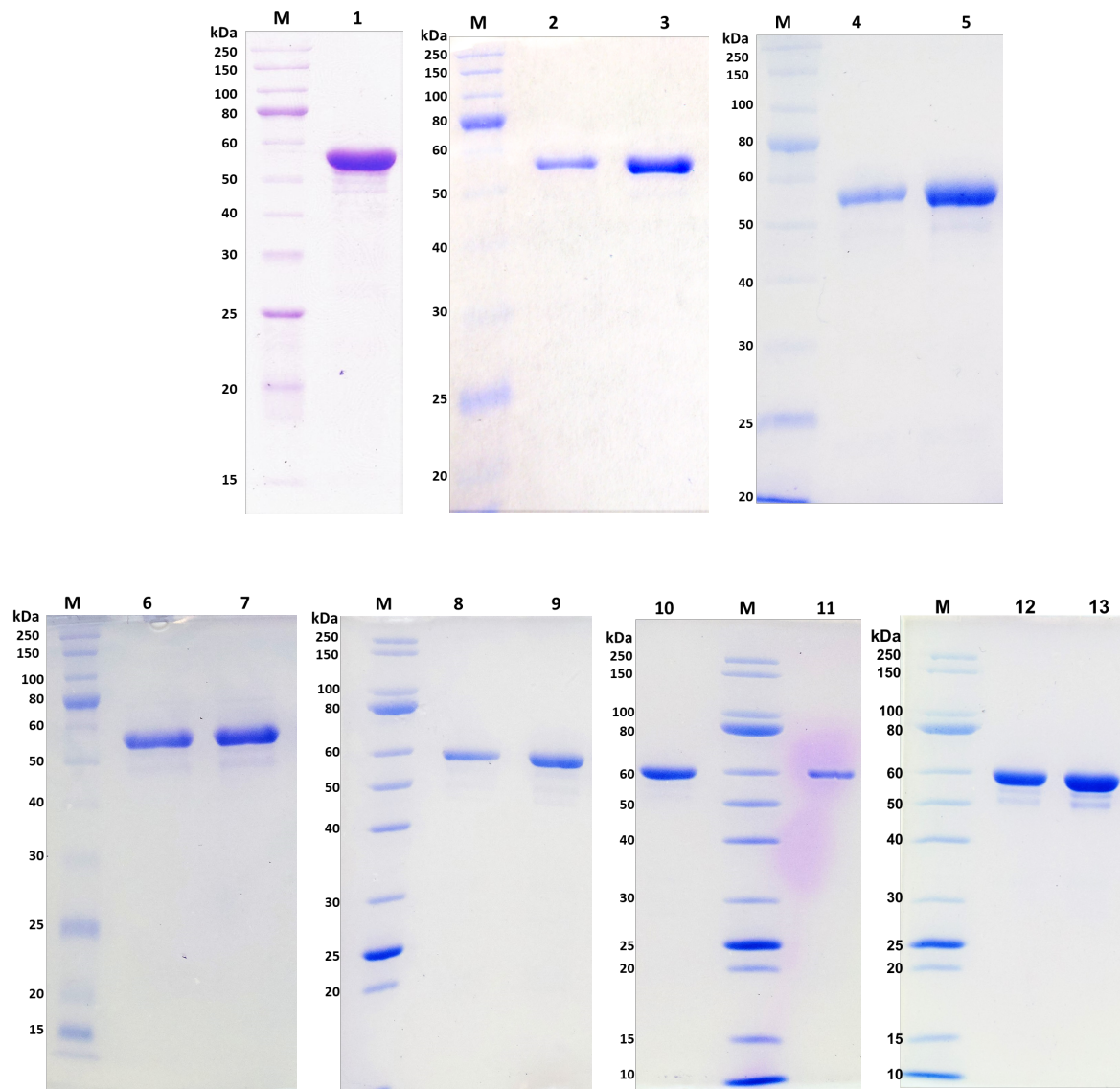
Supplementary Figure 3. Design and Southern analysis of the $\Delta ptmR1/\Delta ptmA1$ double mutant *S. platensis* SB12037. (a) Schematic representation for the deletion of *ptmA1* in *S. platensis* SB12029 by insertion of an *aac(3)IV + oriT* cassette. A probe for *ptmA1* (427 bp), were amplified using genomic DNAs as the template. (b) Southern blot verification of wild-type *ptmA1* (3982 bp) and double crossover $\Delta ptmA1$ (2123 bp) mutant genotypes. Lane 1, DNA marker VII, DIG-labeled (Roche); lane 2, *S. platensis* SB12029; lane 3, *S. platensis* SB12037. Southern analysis ($n=1$) was in agreement with PCR diagnostic experiments.



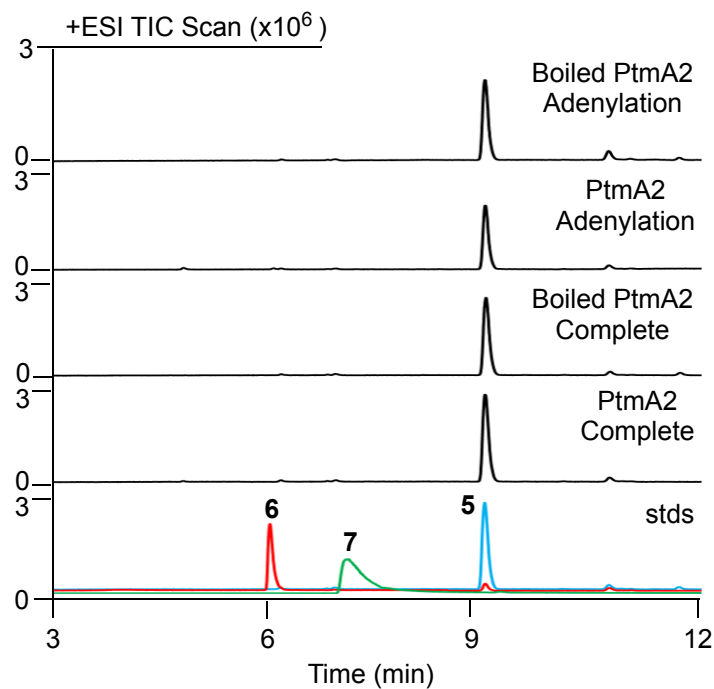
Supplementary Figure 3 cont. Design and Southern analysis of the $\Delta ptmR1/\Delta ptmA2$ double mutant *S. platensis* SB12038. (c) Schematic representation for the deletion of *ptmA2* in *S. platensis* SB12029 by insertion of an *aac(3)IV + oriT* cassette. A probe for *ptmA2* (442 bp), were amplified using genomic DNAs as the template. (d) Southern blot verification of wild-type *ptmA2* (4770 bp) and double crossover $\Delta ptmA2$ (3108 bp) mutant genotypes. Lane 1, *S. platensis* SB12029; lane 2, *S. platensis* SB12038; lane 3, DNA marker VII, DIG-labeled (Roche). Southern analysis ($n=1$) was in agreement with PCR diagnostic experiments.



Supplementary Figure 4. SDS-PAGE of Ptma2 and mutants. Lanes M, Unstained protein ladder (NEB); lane 1, wild-type Ptma2; lanes 2 and 3, Ptma2 H215A; lanes 4 and 5, Ptma2 E416A; lanes 6 and 7, Ptma2 A497K; lanes 8 and 9, Ptma2 P-loop; lanes 10 and 11, Ptma2 A497K/P-loop. The calculated MWs for wild-type Ptma2 and mutants are all approximately ~59.3 kDa. Gels are representative examples of n>3 independent experiments.

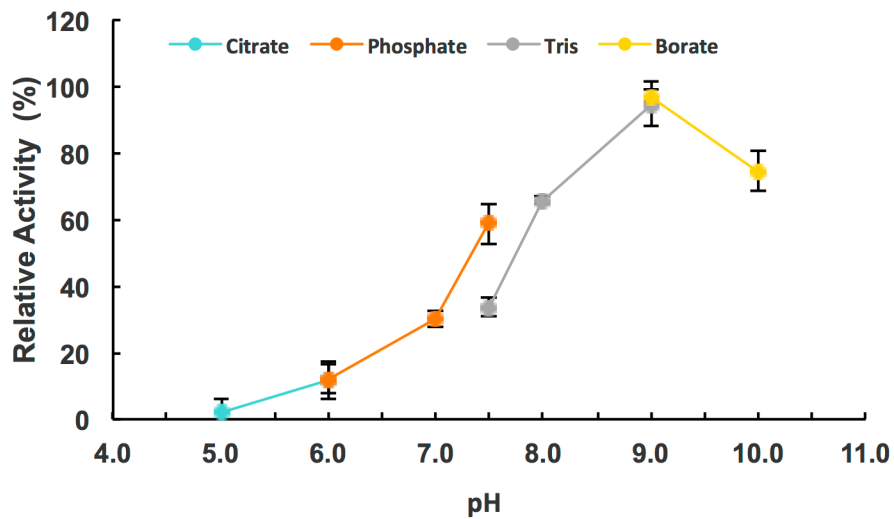


Supplementary Figure 5. Total ion chromatograms (TICs) of PtmA2 enzyme reactions. (Panels) Boiled and enzymatic reactions with PtmA2; (stds) overlaid standards of **5**, **6**, and **7** (color-coded). PtmA2 does not catalyze the first half adenylation reaction or the complete (adenylation and thioesterification) reaction. Chromatograms are representative examples of $n > 3$ independent experiments.

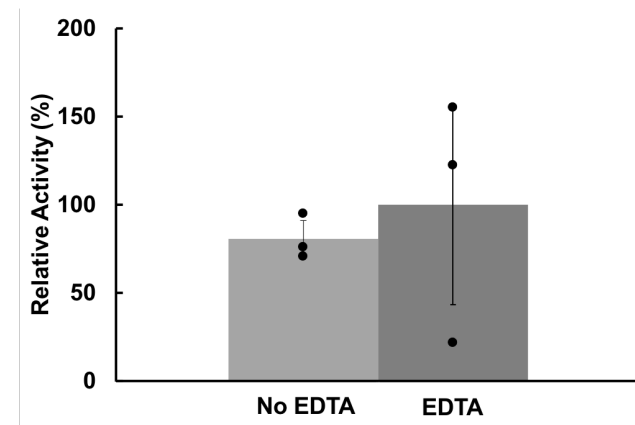


Supplementary Figure 6. PtmA2 reaction optimization. All experiments were performed in triplicate and each data point represents the mean of the three independent assays with error bars representing the standard deviation. (a) Buffer and pH optimization. The relative activity of PtmA2 was calculated in the presence of citrate, phosphate, tris or borate buffer (color-coded) with a total pH range of 5.0 – 10.0. (b) Divalent metal ion dependence. The relative activities of the PtmA2 reaction was calculated with (100%) or without (80%) 10 mM EDTA supporting that PtmA2 does not require divalent metal ions for thioesterification.

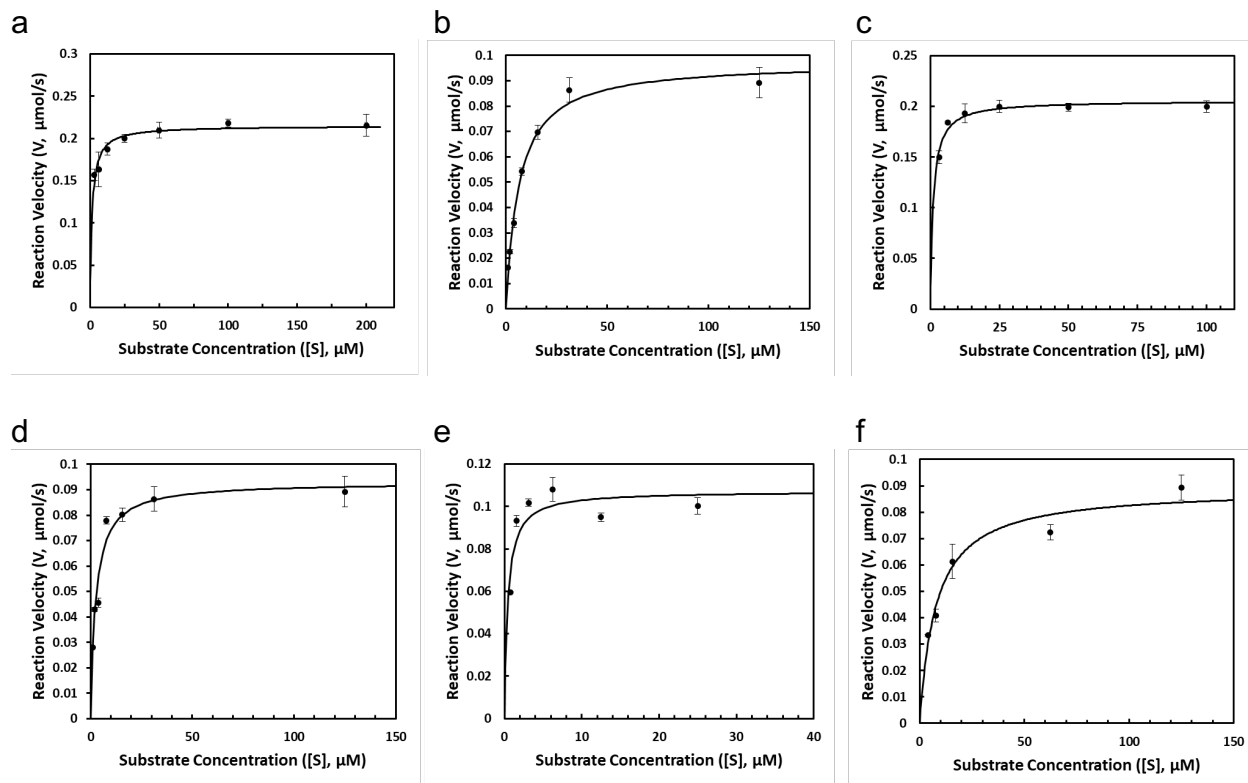
a



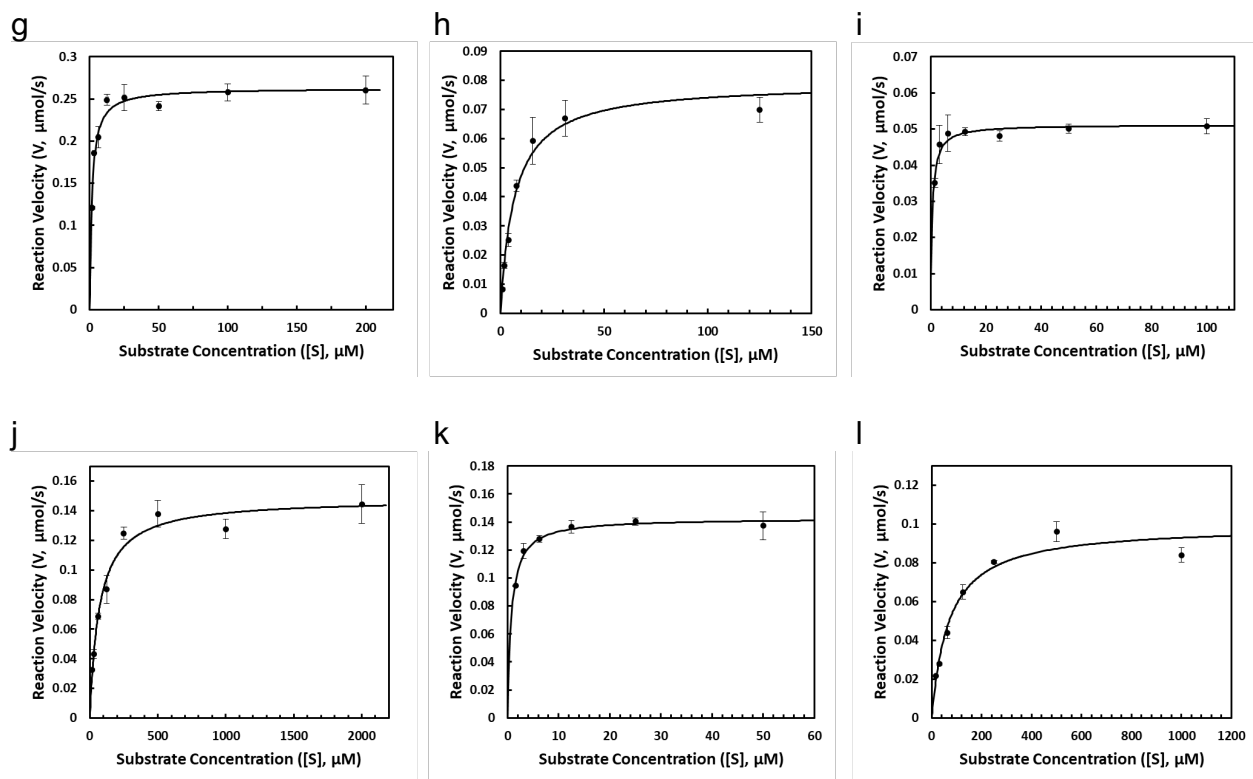
b



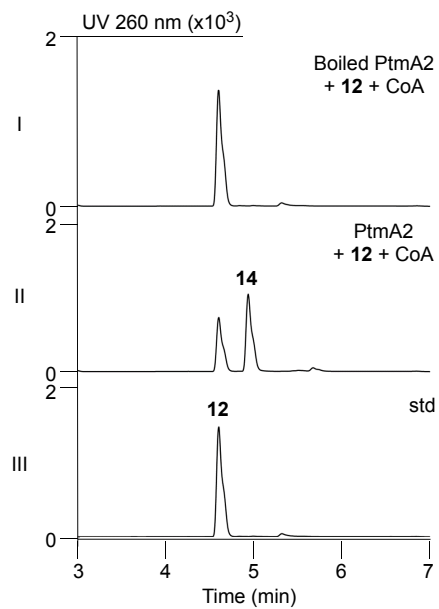
Supplementary Figure 7. Steady-state kinetics of Ptma2 and mutants. Michaelis-Menten plots of rate vs substrate, either diterpenoid adenylate or CoA, concentrations are shown. The determined kinetic parameters are summarized in Table 1. Kinetics were performed in triplicate and each data point represents the mean of the three independent assays with error bars representing the standard deviation. Nonlinear regression was performed using the K_m and V_{max} Tool Kit (ic50.tk/kmvmax.html). (a) native Ptma2 (10 nM) and CoA (2 mM) were incubated with varying concentrations (3–200 μ M) of 6. (b) native Ptma2 (5 nM) and 6 (100 μ M) were incubated with varying concentrations (0.9–125 μ M) of CoA. (c) native Ptma2 (10 nM) and CoA (2 mM) were incubated with varying concentrations (3–100 μ M) of 9. (d) native Ptma2 (5 nM) and 9 (100 μ M) were incubated with varying concentrations (0.9–125 μ M) of CoA. (e) Ptma2 E416A (500 nM) and CoA (2 mM) were incubated with varying concentrations (0.7–25 μ M) of 6. (f) Ptma2 E416A (500 nM) and 6 (100 μ M) were incubated with varying concentrations (3.9–125 μ M) of CoA.



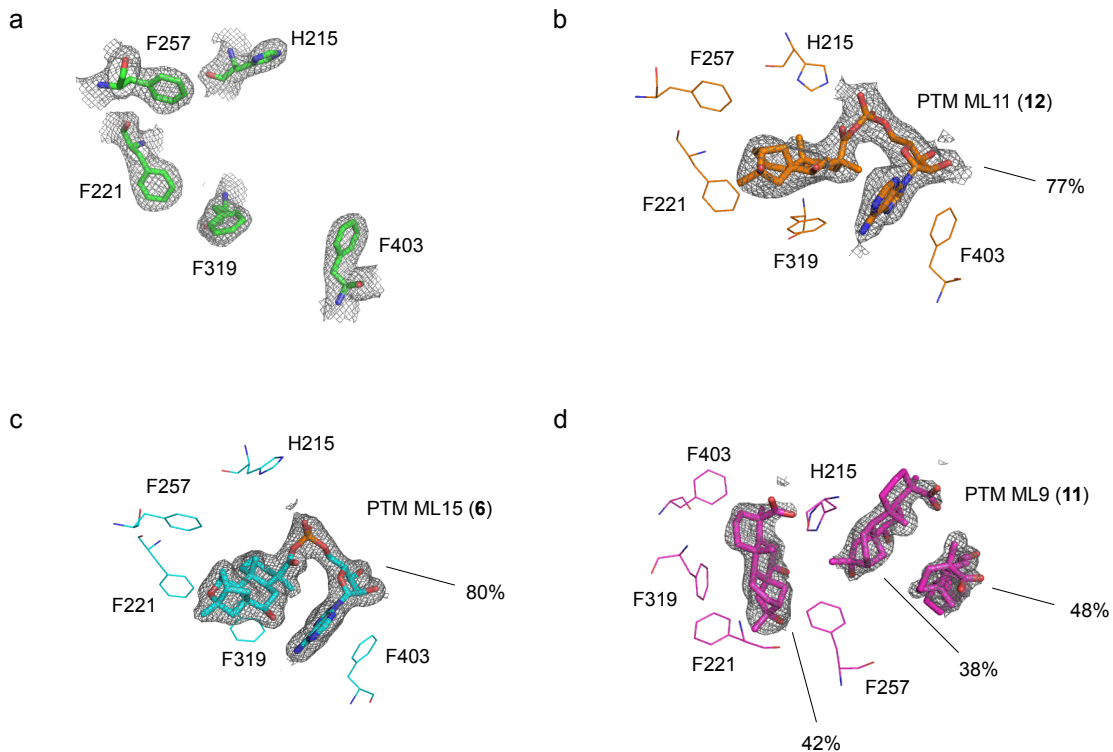
Supplementary Figure 7 cont. Steady-state kinetics of PtmA2 mutants (g) PtmA2 A497K (10 nM) and CoA (2 mM) were incubated with varying concentrations (3–200 μ M) of **6**. (h) PtmA2 A497K (2.5 nM) and **6** (100 μ M) were incubated with varying concentrations (0.9–125 μ M) of CoA. (i) PtmA2 P-loop mutant (5 nM) and CoA (2 mM) were incubated with varying concentrations (1–100 μ M) of **6**. (j) PtmA2 P-loop mutant (20 nM) and **6** (100 μ M) were incubated with varying concentrations (15–2000 μ M) of CoA. (k) PtmA2 A497K/P-loop (10 nM) and CoA (2 mM) were incubated with varying concentrations (1–50 μ M) of **6**. (l) PtmA2 A497K/P-loop (10 nM) and **6** (100 μ M) were incubated with varying concentrations (15–2000 μ M) of CoA.



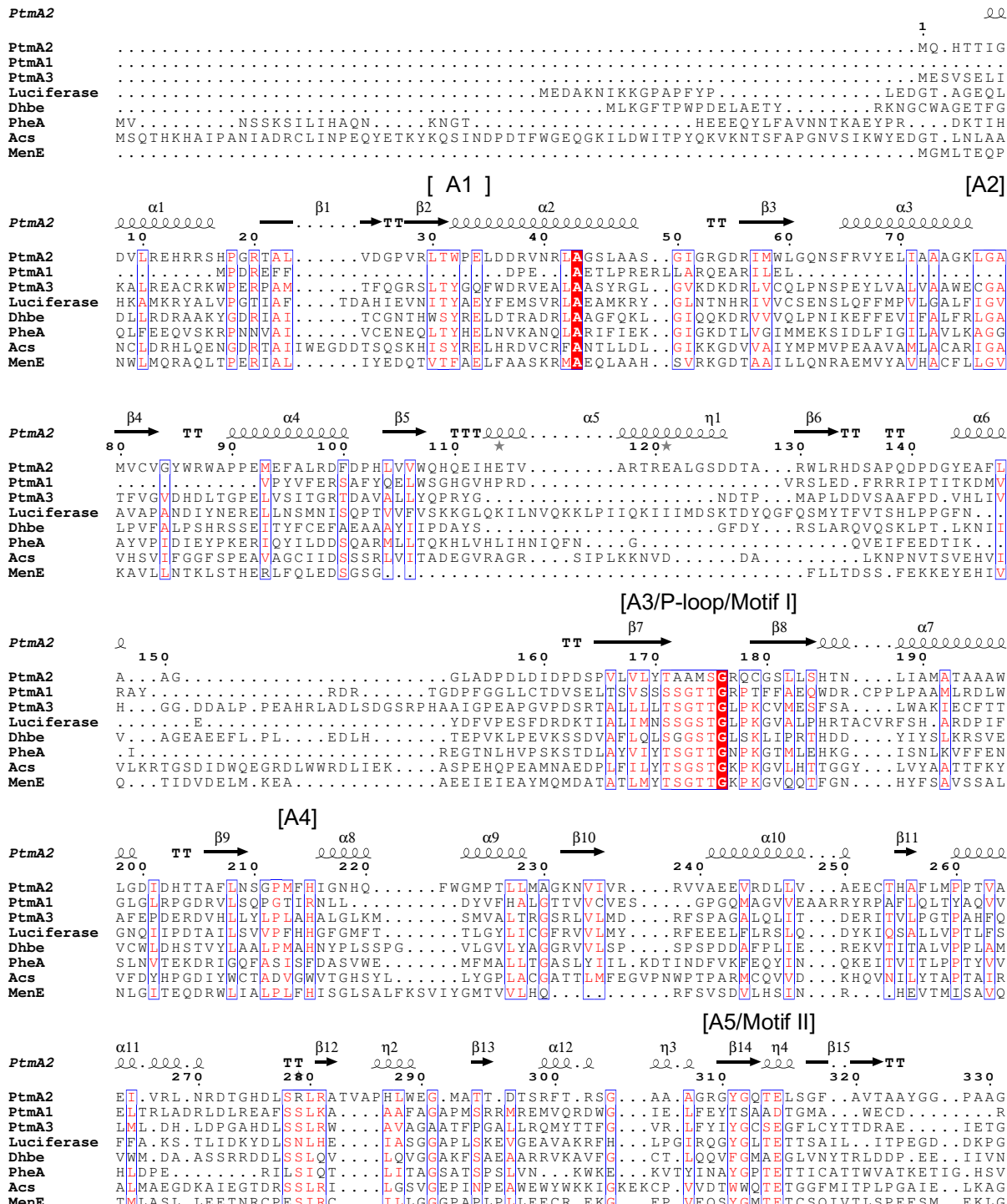
Supplementary Figure 8. HPLC chromatograms of PtmA2 enzyme reactions with nonnative adenylate **12**. (Panels) Adenylate **12** incubated with boiled PtmA2 or PtmA2 yielding CoA thioester **14**; (std) Standard of the “open ether” adenylate **12**. Chromatograms are representative examples of n>3 independent experiments.



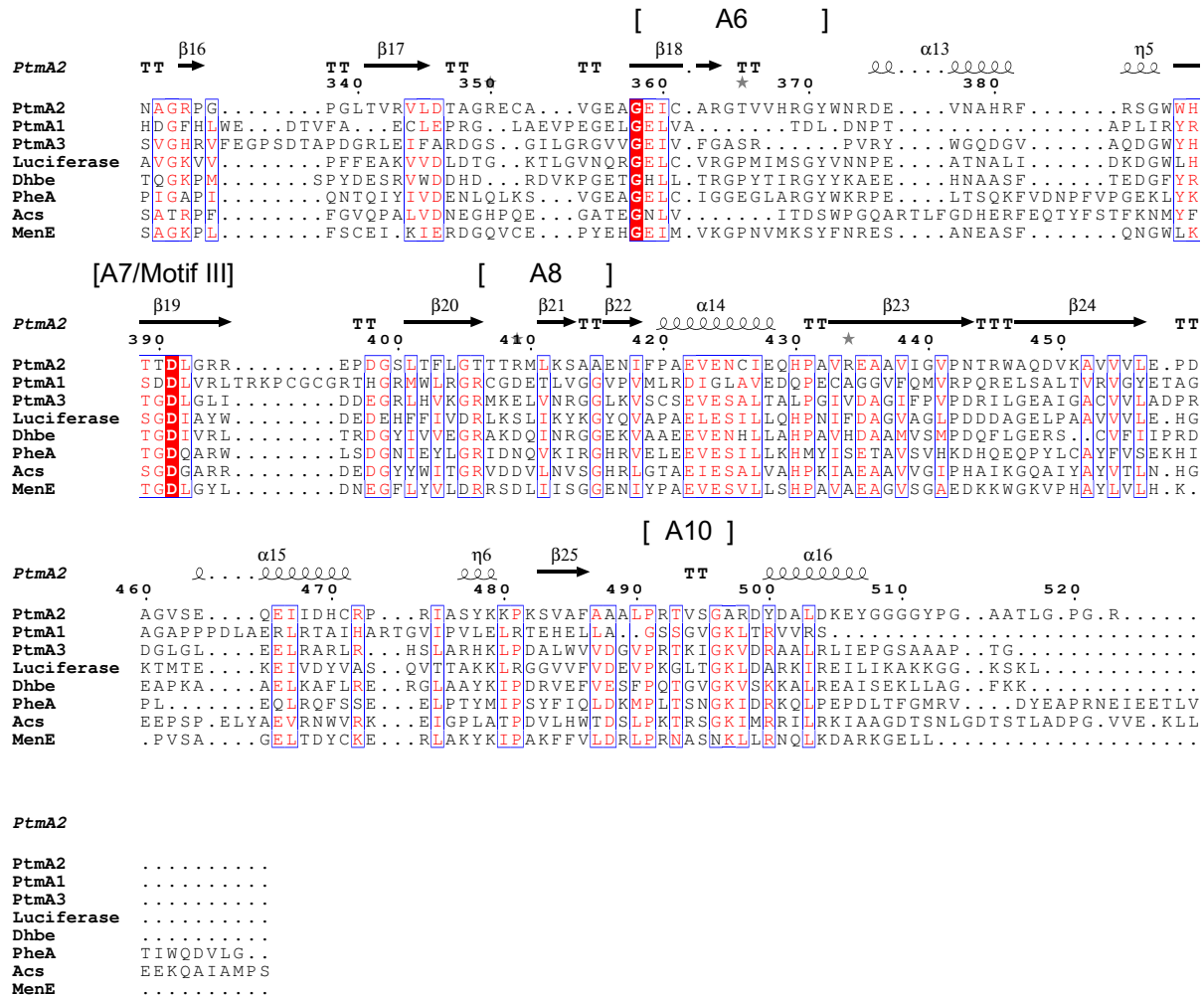
Supplementary Figure 9. Electron density maps for selected active site residues and ligands for unliganded and liganded PtmA2. The $2mF_o - DF_c$ omit maps for (a) active site residues in unliganded PtmA2 (PDB entry 5E7Q), (b) **12** in PtmA2 (5UPQ), (c) **6** in PtmA2 (5UPS), and (d) **11** in PtmA2 (5UPT). A 1.0σ contour and a 2.0 \AA carve are shown in grey. Occupancies of each ligand are shown as percentages.



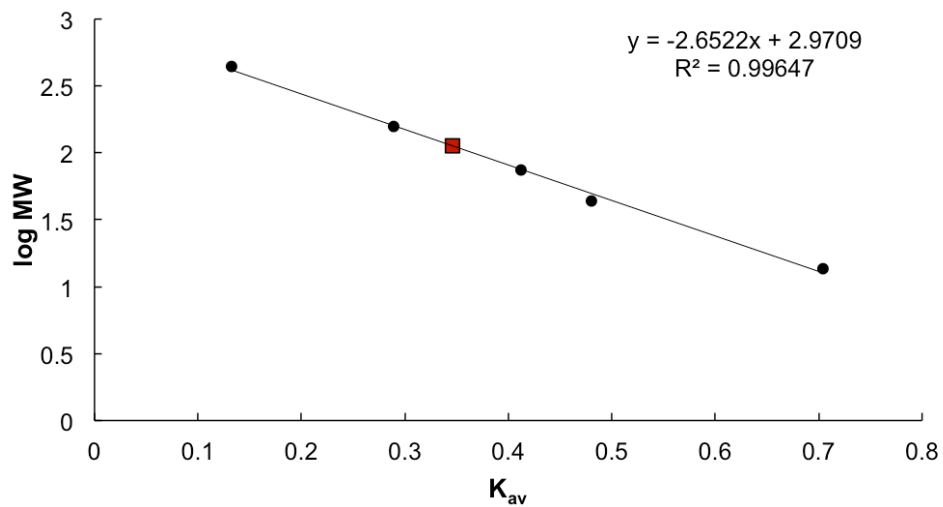
Supplementary Figure 10. Full sequence alignment of PtmA2 and selected acyl-CoA synthetases. Aligned residues are colored based on the level of conservation (red box with white character shows strict identity, red character similarity, and blue frame similarity across groups). The corresponding secondary structure of PtmA2 (739A2, PDB entry 5E7Q) is depicted above the sequence alignment. Core motif sequences (A1–A10)¹¹ and motifs (I–III)¹² are listed in brackets. The alignment was created with MUSCLE¹³ and rendered with ESPript 3.0¹⁴.



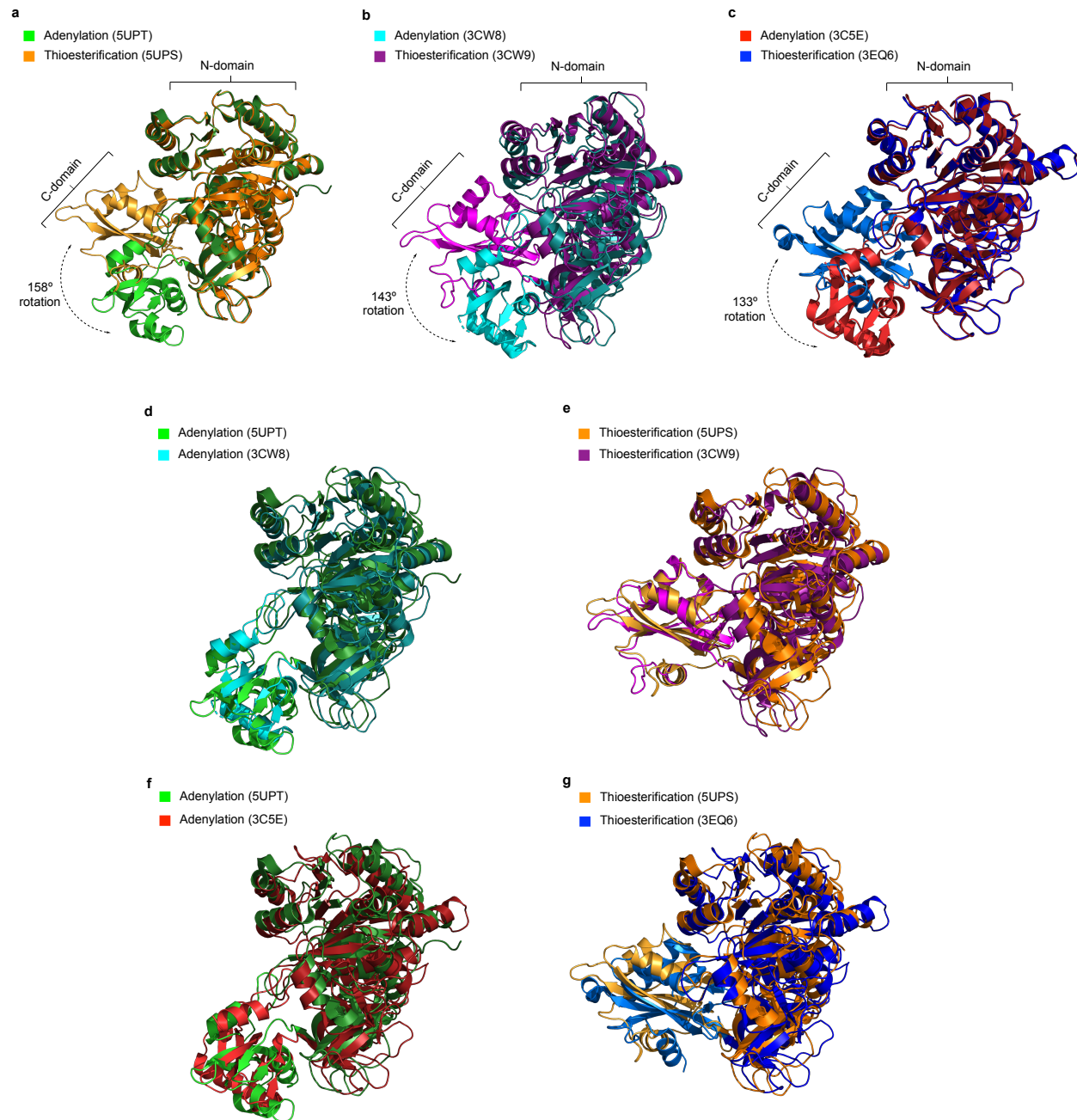
Supplementary Figure 10 cont. Full sequence alignment of Ptma2 and selected acyl-CoA synthetases.



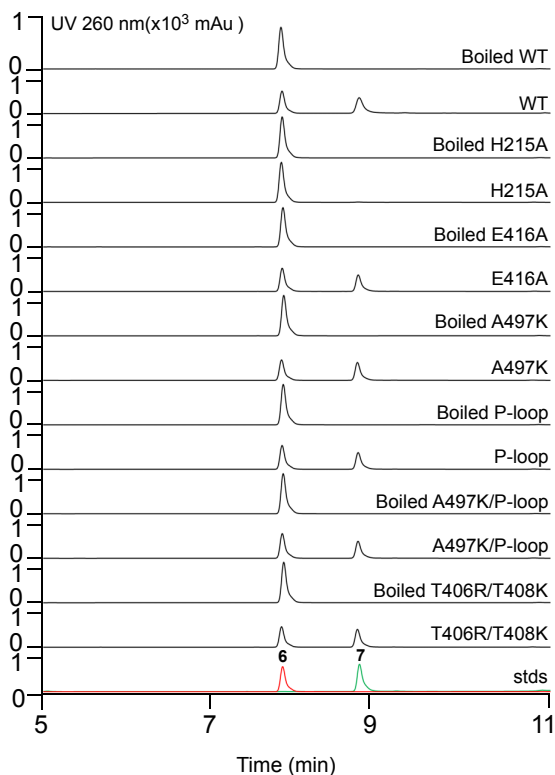
Supplementary Figure 11. Size-exclusion chromatography of PtmA2. Ribonuclease A (13.7 kDa), ovalbumin (44 kDa), conalbumin (75 kDa), aldolase (158 kDa), and ferritin (440 kDa) were used to construct the standard curve (black circles). The calibration curve of K_{av} versus $\log(MW)$ was prepared using the equation $K_{av} = V_e - V_o / (V_t - V_o)$, where V_e , V_o , and V_t is the elution volume, column void volume, and total bed volume, respectively. PtmA2 (red square) eluted at a retention volume of 70.3 mL, correlating to a MW of 112.9 kDa. The calculated MW for His₆-tagged PtmA2 is ~59.3 kDa. Size-exclusion chromatography was performed n=1 for native PtmA2; the elution volume, and thus calculated MW was consistent with size-exclusion chromatography of selected PtmA2 mutants.



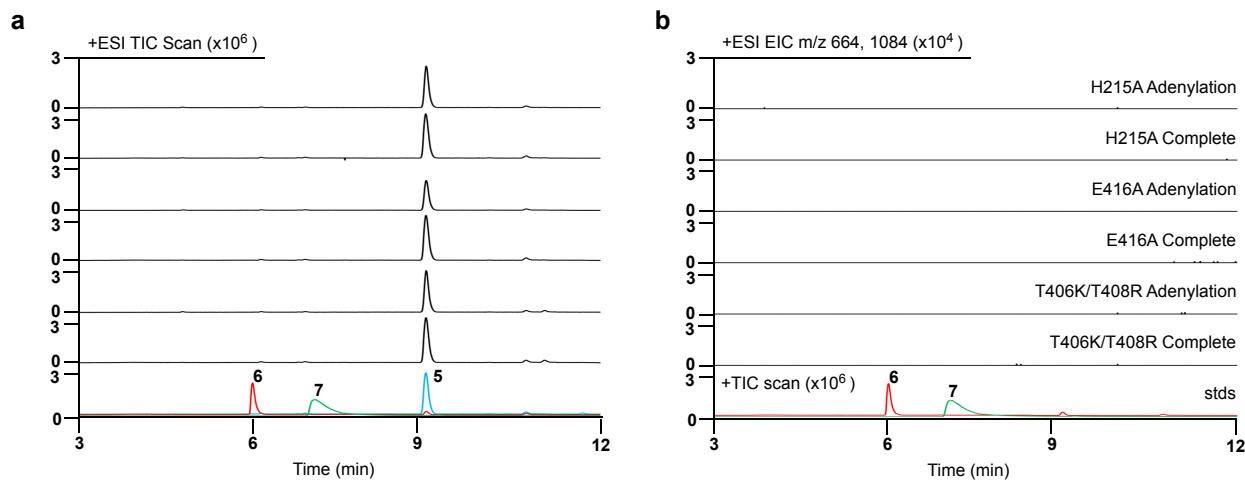
Supplementary Figure 12. Domain alterations of PtmA2 and selected members of the ANL superfamily. (a-c) Superposition of the adenylation and thioesterification conformations of PtmA2, *Alcaligenes* sp. 4-chlorobenzoyl-CoA ligase (CBL)¹⁵, and human medium chain acyl-CoA synthetase (hACS)¹⁶, respectively. The N and C-terminal domains, which are shown in dark and light colors, respectively, rotate 158°, 143°, 133°, respectively. (d) Superposition of the adenylation conformations of PtmA2 and CBL. (e) Superposition of the thioesterification conformations of PtmA2 and hACS. (f) Superposition of the thioesterification conformations of PtmA2 and CBL. (g) Superposition of the thioesterification conformations of PtmA2 and hACS.



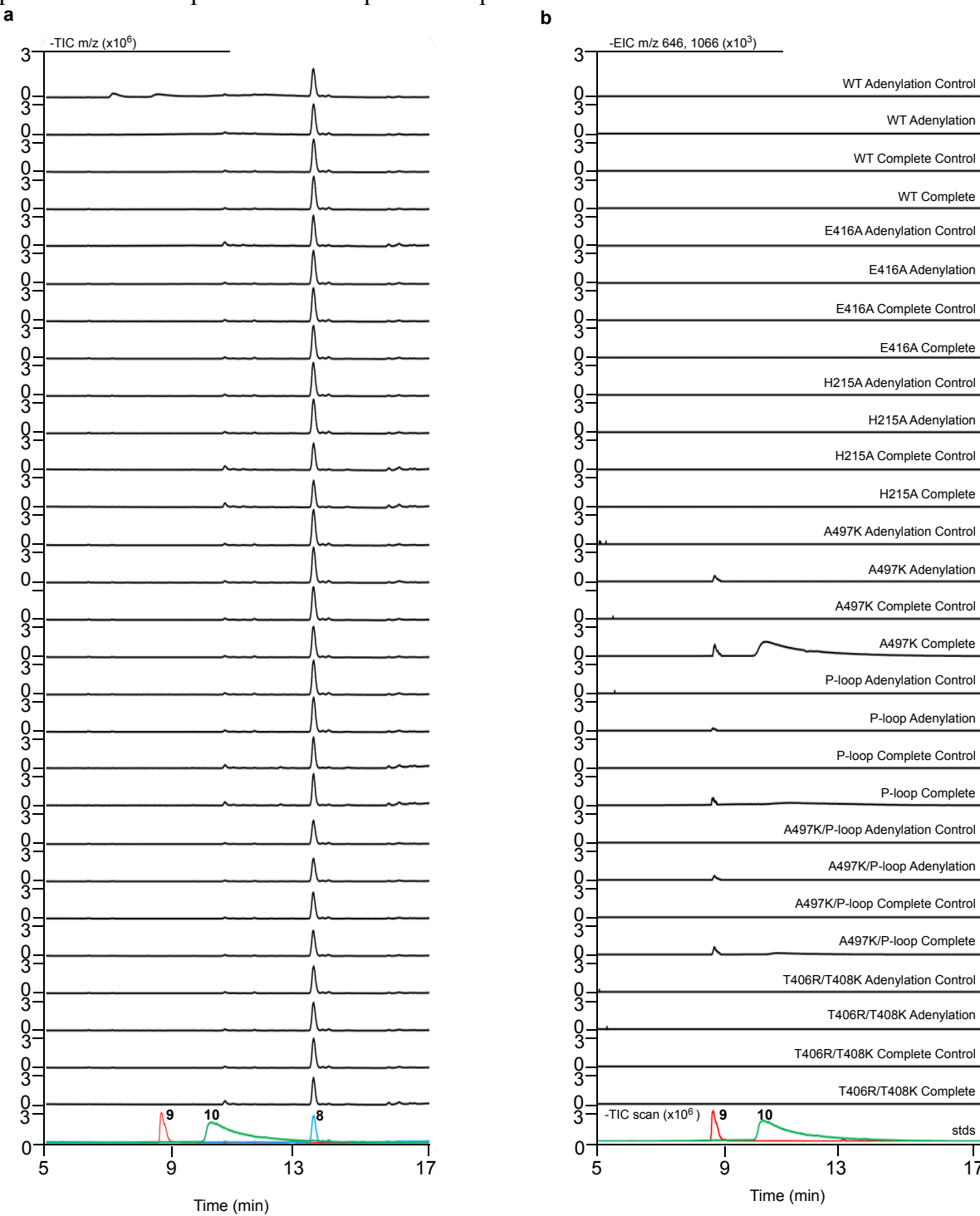
Supplementary Figure 13. HPLC chromatograms of PtmA2 mutant thioesterification reactions. (Panels) Adenylate **6** incubated with boiled PtmA2 variants or PtmA2 variants; (stds) overlaid standards of **6** and **7** (color-coded). Chromatograms are representative examples of n>3 independent experiments.



Supplementary Figure 14. LC-MS chromatograms of PtmA2 mutant reactions. (a) Total ion chromatograms (TICs) and (b) extracted ion chromatograms (EICs) of PtmA2 mutant enzyme reactions. (Panels) Adenylation and complete (both adenylation and thioesterification) reactions with native and mutant PtmA2; (stds) overlaid standards of 5, 6, and 7 (color-coded). See Supplementary Figs. 15 and 17 for reactions using free acid **8** and negative controls using boiled PtmA2, respectively. Chromatograms are representative examples of $n > 3$ independent experiments.



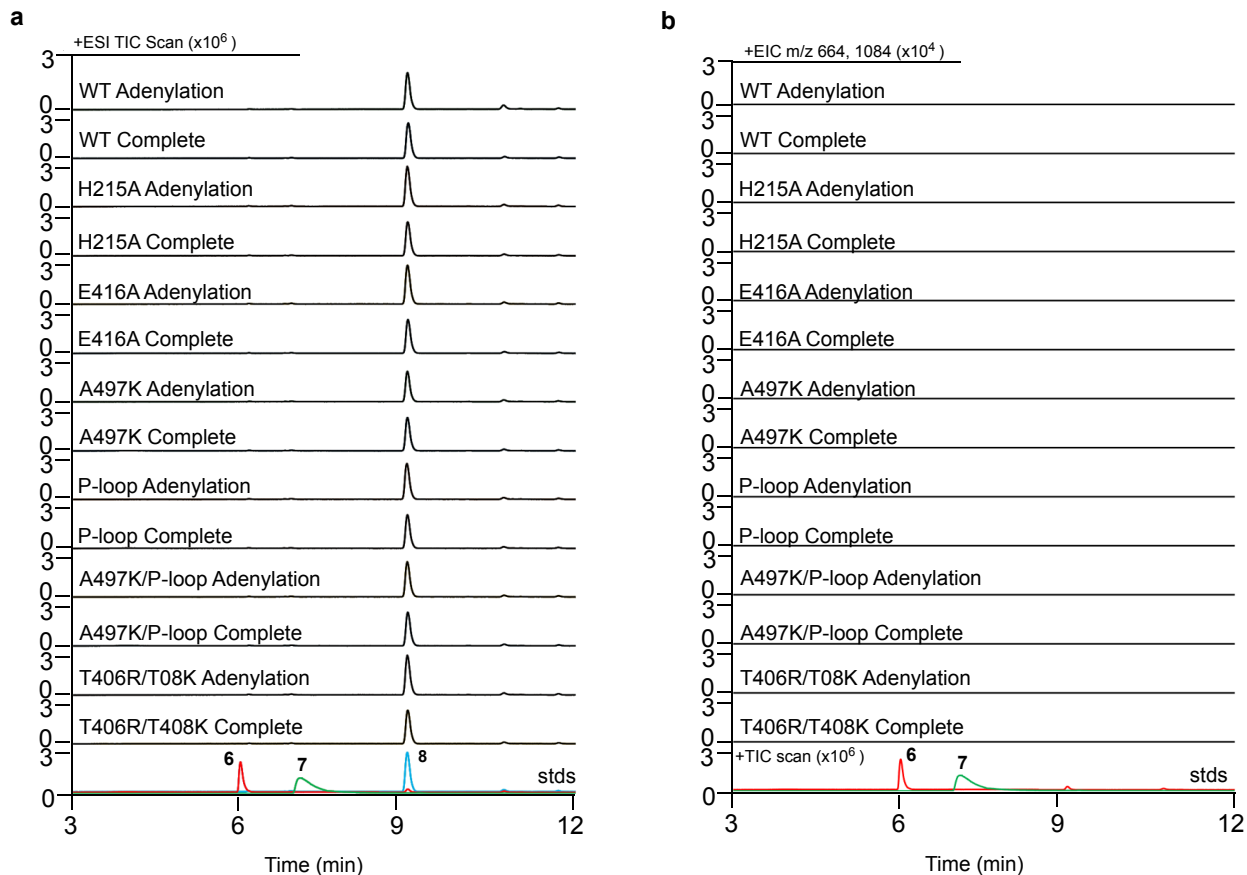
Supplementary Figure 15. Conversion of free acid **8** to CoA thioester **10** using PtmA2 mutants. (a) Total ion chromatograms (TICs) and (b) extracted ion chromatograms (EICs) of each PtmA2 mutant enzyme reaction. (Panels) Adenylation and complete reactions, along with boiled enzyme negative controls, with native and mutant PtmA2; (stds) overlaid standards of **8**, **9**, and **10** (color-coded). Adenylation reactions were incubated with free acid **8**, ATP, and Mg²⁺; complete reactions were incubated with free acid **8**, ATP, Mg²⁺, and CoA. Chromatograms are representative examples of n>3 independent experiments.



Supplementary Figure 16. Sequence alignment of PtmA2 and selected PtmA2-like acyl-CoA ligases. A3 (P-loop), A4, A8, and A10 core motifs are shown. All selected homologues are from gram-positive bacteria with protein sequence identities ranging from 67–97%.

		A3 (P-loop)		A4		A8		A10
PtmA2	168	VLYTAAMSGRQCG	...	212	PMFHIGN	...	406	TTRMLKSAAE
PtnA2	168	VLYTAAMSGRQCG	...	212	PMFHIGN	...	406	TTRMLKSAAE
WP_053210057.1	168	VLYTAAMSGRQCG	...	212	PMFHIGN	...	406	TTRMLKSAAE
WP_030985283.1	168	VLYTAAMSGRQCG	...	212	PMFHIGN	...	406	TTRMLKSAAE
WP_033318305.1	175	VIYTAAITGRQSG	...	219	PMFHIGN	...	413	TTRMLKSAAE
WP_055612017.1	174	VIYTAAITGRQSG	...	218	PMFHIGN	...	412	TTRMLKSAAE
WP_030660837.1	169	VIYTAISGRQSG	...	213	PMFHIGN	...	407	TTRMLKSAAE
WP_030927792.1	169	VIYTAISGRQSG	...	213	PMFHIGN	...	407	TTRMLKSAAE
WP_043677510.1	169	VIYTAISGRQSG	...	213	PMFHIGN	...	407	TTRMLKSAAE
WP_020120457.1	184	VIYTAISGRQSG	...	228	PMFHIGN	...	422	TTRMLKSAAE
EDY54705.1	163	VIYTAISGRQSG	...	207	PMFHIGN	...	401	TTRMLKSAAE
WP_037902523.1	169	VIYTAISGRQSG	...	213	PMFHIGN	...	407	TTRMLKSAAE
WP_057582384.1	169	VIYTAISGRQSG	...	213	PMFHIGN	...	407	TTRMLKSAAE
WP_037709893.1	169	VIYTAISGRQSG	...	213	PMFHIGN	...	407	TTRMLKSAAE
WP_031055094.1	169	VIYTAISGRQSG	...	213	PMFHIGN	...	407	TTRMLKSAAE
WP_062039429.1	174	VIYTAISGRQSG	...	218	PMFHIGN	...	412	TTRMLKSAAE
WP_057612788.1	169	VIYTAISGRQSG	...	213	PMFHIGN	...	407	TTRMLKSAAE
WP_059203844.1	169	VIYTAISGRQSG	...	213	PMFHIGN	...	407	TTRMLKSAAE
WP_033278459.1	169	VIYTAISGRQSG	...	213	PMFHIGN	...	407	TTRMLKSAAE
WP_020639301.1	173	VIYTAAMSGTQCG	...	217	PMFHIGN	...	411	TTRMLKSAAE
WP_013225717.1	174	VIYTAAMSGSQCG	...	218	PMFHIGN	...	412	TTRMLKSAAE

Supplementary Figure 17. LC-MS chromatograms of boiled PtmA2 mutant enzyme reactions. See Fig. 5b, 5c and Supplementary Fig. 14 for reaction comparisons. (a) Total ion chromatograms (TICs) and (b) extracted ion chromatograms (EICs) of each reaction. Chromatograms are representative examples of $n > 3$ independent experiments.



Supplementary Information References

1. Gust, B., Challis, G.L., Fowler, K., Kieser, T. & Chater, K.F. PCR-targeted *Streptomyces* gene replacement identifies a protein domain needed for biosynthesis of the sesquiterpene soil odor geosmin. *Proc. Natl. Acad. Sci. U. S. A.* **100**, 1541–1546 (2003).
2. Cherepanov, P.P. & Wackernagel, W. Gene disruption in *Escherichia coli*: TcR and KmR cassettes with the option of FLP-catalyzed excision of the antibiotic-resistance determinant. *Gene* **158**, 9–14 (1995).
3. MacNeil, D.J. et al. Analysis of *Streptomyces avermitilis* genes required for avermectin biosynthesis utilizing a novel integration vector. *Gene* **111**, 61–68 (1992).
4. Rudolf, J.D., Dong, L.-B., Huang, T. & Shen, B. A genetically amenable platensimycin- and platencin-overproducer as a platform for biosynthetic explorations: a showcase of PtmO4, a long-chain acyl-CoA dehydrogenase. *Mol. BioSyst.* **11**, 2717–2726 (2015).
5. Lohman, J.R., Bingman, C.A., Phillips, G.N. & Shen, B. Structure of the bifunctional acyltransferase/decarboxylase LnmK from the leinamycin biosynthetic pathway revealing novel activity for a double-hot-dog fold. *Biochemistry* **52**, 902–911 (2013).
6. Eschenfeldt William, H. et al. New LIC vectors for production of proteins from genes containing rare codons. *J. Struct. Funct. Genomics* **14**, 135–144 (2013).
7. Rudolf, J.D., Dong, L.-B., Manoogian, K. & Shen, B. Biosynthetic origin of the ether ring in platensimycin. *J. Am. Chem. Soc.* **138**, 16711–16721 (2016).
8. Smanski, M.J. et al. Expression of the platencin biosynthetic gene cluster in heterologous hosts yielding new platencin congeners. *J. Nat. Prod.* **75**, 2158–2167 (2012).
9. Smanski, M.J. et al. Dedicated *ent*-kaurene and *ent*-atiserene synthases for platensimycin and platencin biosynthesis. *Proc. Natl. Acad. Sci. U. S. A.* **108**, 13498–13503 (2011).
10. Hindra et al. Strain prioritization for natural product discovery by a high-throughput real-time PCR method. *J. Nat. Prod.* **77**, 2296–2303 (2014).
11. Marahiel, M.A., Stachelhaus, T. & Mootz, H.D. Modular peptide synthetases involved in nonribosomal peptide synthesis. *Chem. Rev.* **97**, 2651–2673 (1997).
12. Chang, K.-H., Xiang, H. & Dunaway-Mariano, D. Acyl-adenylate motif of the acyl-adenylate/thioester-forming enzyme superfamily: a site-directed mutagenesis study with the *Pseudomonas* sp. strain CBS3 4-chlorobenzoate:coenzyme A ligase. *Biochemistry* **36**, 15650–15659 (1997).
13. Edgar, R.C. MUSCLE: multiple sequence alignment with high accuracy and high throughput. *Nucleic Acids Res.* **32**, 1792–1797 (2004).
14. Gouet, P., Courcelle, E., Stuart, D.I. & Metoz, F. ESPript: analysis of multiple sequence alignments in PostScript. *Bioinformatics* **15**, 305–308 (1999).
15. Reger, A.S., Wu, R., Dunaway-Mariano, D., & Gulick, A.M. Structural characterization of a 140 degree domain movement in the two-step reaction catalyzed by 4-chlorobenzoate:CoA ligase. *Biochemistry* **47**, 8016–8025 (2008).
16. Kochan, G., Pilka, E.S., von Delft, F., Opperman, U. & Yue, W.W. Structural snapshots for the conformation-dependent catalysis by human medium-chain acyl-coenzyme A synthetase ACSM2A. *J. Mol. Biol.* **388**, 997–1008 (2009).